Implicit Z_{bus} Gauss Algorithm Revisited

Fei Feng, *Student Member, IEEE*, and Peng Zhang, *Senior Member, IEEE*

***Abstract*—The implicit Z_{bus} Gauss algorithm is revisited to empower the power flow analysis for microgrids with hierarchical control and frequency- and voltage- dependent loads. The contributions of the revisited Gauss (GRev) algorithm include: 1) a droop-based implicit Z_{bus} Gauss microgrid algorithm which automatically incorporates the distributed energy resources (DERs)/load droop effects; 2) new formulations which accurately integrate the secondary control adjustments for power sharing and voltage regulation. Case studies verify the efficacy, robustness and excellent convergence performance of GRev for both radial and meshed microgrids.**

***Index Terms*—Microgrid power flow, implicit Z_{bus} Gauss, hierarchical control, droop.**

I. Introduction

THE unprecedentedly frequent blackouts, e.g. the rolling outages caused by California fires, signal the urgent need to modernize today's fragile power infrastructure by increasing the penetration of microgrids. To enable resilient and efficient microgrids, microgrid power flow is a keystone function which is indispensable for the microgrid planning and energy management.

Power flow of islanded microgrids remains an open challenge because: 1) a slack bus no longer exists 2) distributed energy resources (DERs) and loads are regulated by droop/secondary controls, and 3) microgrid configuration and control schemes vary frequently. Backward/forward sweep (BFS) has been modified for droop-based microgrid [1], microgrid with secondary control [2], and networked microgrids [3], which, however, cannot handle meshed microgrids. Newton's method [4] is extended to consider the droop control, whereas it is unable to handle hierarchical controls.

To address the challenge above, this letter devises a revisited implicit Z_{bus} Gauss algorithm (GRev) which is able to handle arbitrary structures and allows incorporating DER hierarchical controls as well as load droops. Besides, GRev is more robust than Newton's method because of its insensitivity to initial values. Thus, GRev is particularly useful for meshed microgrids for urban and populated communities or mission-critical microgrids requiring higher reliability and resilience.

Manuscript received November 27, 2019; revised March 13, 2020; accepted May 25, 2020. Date of publication June 8, 2020; date of current version August 24, 2020. This work was supported by the National Science Foundation under Grant ECCS-1831811. Paper no. PESL-00278-2019. *(Corresponding author: Peng Zhang.)*

The authors are with the Department of Electrical and Computer Engineering, Stony Brook University, Stony Brook, NY 11794-2350 USA (e-mail: fei.feng@stonybrook.edu; P.Zhang@stonybrook.edu).

Color versions of one or more of the figures in this article are available online at https://ieeexplore.ieee.org.

Digital Object Identifier 10.1109/TPWRS.2020.3000658

II. Implicit Z_{BUS} Gauss Algorithm Revisited

Impilicit Z_{bus} Gauss (Z_{bus}) is a fixed-point algorithm which exploits the sparse Y_{bus} matrix and equivalent current superposition to solve the network equations [5]. As DERs cannot hold the voltages and frequency constant in an islanded microgrid, we introduce a bus type called *DER buses* to which those DERs equipped with hierarchical controls are connected. Different from the traditional PV buses or slack bus, the DER buses absorb the mismatch between generation and demand in an islanded microgrid by regulating the system frequency and bus voltages. One of the DER buses is selected as a leader bus for updating the frequency.

A. Basic GRev Formulation

The DER power injections are determined by a two-layer hierarchical control system [6]. Therefore, the GRev power flow for an N-bus microgrid with DER hierarchical control and load droops are formulated as:

$$\begin{bmatrix}\mathbf{I}_E(\mathbf{V}_E,f)\\ \mathbf{I}_S(\mathbf{V}_S,f)\end{bmatrix}=\begin{bmatrix}\mathbf{Y}_{EE}\mathbf{Y}_{ES}\\ \mathbf{Y}_{SE}\mathbf{Y}_{SS}\end{bmatrix}\begin{bmatrix}\mathbf{V}_E\\ \mathbf{V}_S\end{bmatrix} \tag{1}$$

$$\mathbf{I}_E(\mathbf{V}_E,f)=\Big[conj(\mathbf{S}_E(\mathbf{V}_E,f)/\mathbf{V}_E)\Big] \tag{2}$$

where $\mathbf{I}_S$ and $\mathbf{V}_S$ are the current and voltage of the DER bus designated for updating the frequency, respectively; $\mathbf{I}_E$ and $\mathbf{V}_E$ are those of the remaining buses; $\mathbf{Y}_{EE}$, $\mathbf{Y}_{SS}$, $\mathbf{Y}_{SE}$ and $\mathbf{Y}_{ES}$ are the admittance submatrices; $\mathbf{S}_E(\mathbf{V}_E,f)=(\mathbf{P_G}(f)-\mathbf{P_L}(f))+j(\mathbf{Q_G}(\mathbf{V}_E)-\mathbf{Q_L}(\mathbf{V}_E))\in\mathbb{C}^{(N-1)\times 1}$ is the power injection (generation minus load) vector. Different from the Z_{bus} method, in the GRev algorithm $\mathbf{I}_{E,S}$ vary with $\mathbf{V}_{E,S}$ and the system frequency f, and $\mathbf{V}_S$ is no longer constant.

The iterative formula for updating $\mathbf{V}_E$ can then be derived from (1-2), as follows

$$\mathbf{V}_E=\Big[\mathbf{Y}_{EE}^{-1}\cdot(\mathbf{I}_E(\mathbf{V}_E,f))-\mathbf{Y}_{ES}\cdot\mathbf{V}_S)\Big] \tag{3}$$

B. GRev With Hierarchical Control

The GRev algorithm consists of a double-loop iteration process (see **Algorithm 1**). Whenever the nodal power injections update, the bus voltages will subsequently be refreshed. The power updating loop depends upon the hierarchical control modes. Assuming that the P/F and Q/V droop coefficients of DERs and loads are $\mathbf{m_G}$, $\mathbf{n_G}$, $\mathbf{m_L}$, $\mathbf{n_L}$, respectively. Under the

Algorithm 1: GRev Algorithm.

Initialize: $\mathbf{V_{E,S}}$, f, ξ, ρ(RPS/ST), $\mathbf{V}_d$(VR/ST), $\mathbf{Z}_d$(VR/ST);
while $\Delta\mathbf{V_S}$, $\Delta\rho$(RPS/ST), $\Delta\mathbf{V}_d$(VR/ST)$\geq\xi$ **do**
  Update: $imag(\Delta\mathbf{S_E})$, $\Delta\mathbf{Q_E}$ (RPS/ST),$\Delta\mathbf{Q_{ES}}$ (VR/ST)**Eq.**(4,5,6);
  while $\Delta f\geq\xi$ **do**
    Update: $real(\Delta\mathbf{S_E})$, $\Delta\mathbf{P_E}$ **Eq.**(4);
    while $\Delta\mathbf{V_E}\geq\xi$ **do**
      $\mathbf{V_E}$ **Eq.**(1,2,3);
    end
    Update: $\Delta\mathbf{V_S}$, Δf, ρ(RPS/ST), $\mathbf{V}_d$(VR/ST) **Eq.**(7,8);
  end
end
Result: $\mathbf{V_{E,S}}$, f and the branch power flows.

droop control, nodal injections can be updated as follows

$$\Delta\mathbf{S_E} = \Big[(\mathbf{A}\circ\frac{1}{\mathbf{m_G}} - \mathbf{B}\circ\frac{1}{\mathbf{m_L}})\Delta f + j(\mathbf{A}\circ\frac{1}{\mathbf{n_G}} - \mathbf{B}\circ\frac{1}{\mathbf{n_L}})\Delta\mathbf{V_E}\Big] \quad (4)$$

where $\mathbf{A}$ and $\mathbf{B}$ are the 0/1-status matrices of DERs and loads, respectively; the 0/1-status matrices indicate the connections between DERs/loads and microgrid. When the DER is connected with microgrid, the corresponding matrix element is set as 1; otherwise, 0; and $\circ$ denotes the Hadamard product.

On top of the droop scheme, the secondary control accounts for power sharing and voltage adjustment. Real power increments can be redistributed among DERs when loads recover to the nominal status, following $\Delta\mathbf{P_E} = \Delta f/\mathbf{m_G}$. Without loss of generality, the updating of the DER var outputs under three typical secondary control modes [5] are expressed below:

1) Reactive Power Sharing Mode (RPS): In the RPS mode, all the other DERs adopt the reactive power ratio of the leader DER. $\mathbf{V_S}$ is refreshed according to the Q/V droop. The incremental var outputs $\Delta\mathbf{Q_E}$ can then be expressed by:

$$\Delta\mathbf{Q_E} = \Big[\rho\mathbf{A}\circ{\mathbf{Q_E}}^* - \mathbf{B}\circ\tfrac{1}{\mathbf{n_L}}\Delta\mathbf{V_E} - \mathbf{Q}_{E0}\Big] \quad (5)$$

where the reactive power ratio $\rho = Q_S/Q_S^*$, and ${\mathbf{Q_E}}^*$ denotes the rated var outputs of the follower buses.

2) Voltage Regulation Mode (VR): VR aims to recover the DER bus voltages back to their rated values. Mathematically, the var updates of the DER buses are below:

$$\Delta\mathbf{Q_{E,S}} = \Big[\mathbf{A}\circ diag(\mathbf{V_{E,S}})diag(\mathbf{Z}_d^{-1})(\mathbf{V}_d + \mathbf{V_{E,S}} - 2\mathbf{V_{E,S}}) - \mathbf{B}\circ\frac{1}{\mathbf{n_L}}\Delta\mathbf{V_{E,S}}\Big] \quad (6)$$

In this mode, a dummy bus vector with voltages $\mathbf{V}_d$ is used to adjust var injections for the DER buses. Dummy bus voltage considers the difference between the DER voltage and its rated value. If the DER voltage deviates from the rated value, the deviation will be added up to the dummy bus voltage to adjust the DER var output based on Equation (6). A sensitivity vector $\mathbf{Z}_d$ represents the var differences with respect to the voltage differences between dummy buses and the corresponding DER buses. Here ${\mathbf{V_{E,S}}}^*$ denotes the rated voltages, and the detailed procedure to update $\mathbf{V}_d$ can be found in [3].

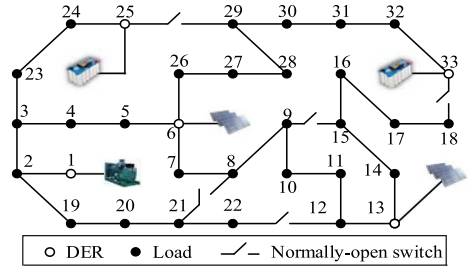

Fig. 1. The 33-bus islanded microgrid with 5 DERs (leader bus: 1).

3) Smart Tuning Mode (ST): One DER bus adopts the VR mode while others follow the RPS mode.

As for the bus voltage updating, once $\mathbf{S}_E(\mathbf{V}_E, f)$ is updated, $\mathbf{V_E}$ can be calculated by (2-3). Then the leader DER bus will update its voltage and the system frequency, as follows,

$$\Delta f = \big[real(conj(\mathbf{V_S}(\mathbf{Y}_{SS}\mathbf{V_S} + \mathbf{Y}_{ES}\mathbf{V_E})) - \mathbf{P_{loss}})/\mathbf{m_G}\big] \quad (7)$$

$$\Delta\mathbf{V_S} = \big[imag(conj(\mathbf{V_S}(\mathbf{Y}_{SS}\mathbf{V_S} + \mathbf{Y}_{ES}\mathbf{V_E})) - \mathbf{Q_{loss}})/\mathbf{n_G}\big] \quad (8)$$

The advantage of GRev is its insensitivity to the choice of initial conditions. All initial values for bus voltage and frequency can be set as unit vectors. This is largely because GRev is a fix-point iteration as seen in (1). Besides, GRev does not rely on any assumption of the microgrid structure, making it suitable for microgrids with arbitrary architectures no matter they are radial, meshed, or honeycomb.

III. Case Study

The effectiveness of GRev is validated on a 33-bus microgrid with 5 DERs (see Fig. 1) [7]. For comparison purposes, all parameters are adopted from [3], except for $\mathbf{Z}_d$. The P/F and Q/V droops of the DER buses 1, 6, 13, 25 and 33 use $\mathbf{m_G} = \mathbf{n_G} = [0.05, 1, 0.1, 1, 0.2]^T$. All DER reference power injections are 0.9 + 0.9j p.u. The virtual impedance value is selected as $\mathbf{Z}_d = 0.05$. Test I verifies GRev on a radial microgrid in Fig. 1. Test II focuses on a meshed microgrid by flipping the five switches. GRev is implemented in Matlab on a 64-bit, 3.70 GHz PC.

A. Verification on Microgrid With Hierarchical Controls

The DER power adjustments for the radial and meshed microgrids under the four control modes are summarized in Tables I and II. A few insights can be obtained:

TABLE I
POWER INJECTIONS FROM DERS (P.U.)

Test	DER#	DP	RPS	VR	ST
I	1	2.50+0.93i	2.50+0.93i	2.50-0.89i	2.50+0.93i
	6	0.98+0.91i	0.98+0.93i	0.98+2.93i	0.98+0.93i
	13	1.70+0.89i	1.70+0.93i	1.70+0.03i	1.70+0.93i
	25	0.98+0.90i	0.98+0.93i	0.98+1.55i	0.98+0.93i
	33	1.30+0.95i	1.30+0.93i	1.30+0.96i	1.30+0.93i
II	1	2.50+0.96i	2.50+0.92i	2.50-0.15i	2.50+0.92i
	6	0.98+0.91i	0.98+0.92i	0.98+2.10i	0.98+0.92i
	13	1.70+0.91i	1.70+0.92i	1.70-0.22i	1.70+0.92i
	25	0.98+0.91i	0.98+0.92i	0.98+3.04i	0.98+0.92i
	33	1.30+0.94i	1.30+0.92i	1.30+0.82i	1.30+0.92i

TABLE II
DER ADJUSTMENT UNDER HIERARCHICAL CONTROL

DER#	$\Delta f/\Delta P$(I)/(II)	$\Delta V/\Delta Q$(I)/(II)	ρ_{RPS}(I)/(II)	ρ_{ST}(I)/(II)
1	0.0500/0.0499	0.0502/0.0503	1.0287/1.0275	1.0287/1.0274
6	1.0000/1.0001	1.0014/1.0006	1.0287/1.0275	1.0287/1.0274
13	0.1001/0.0998	0.0983/0.1017	1.0287/1.0275	1.0287/1.0274
25	1.0000/1.0004	1.0015/1.0016	1.0287/1.0275	1.0287/1.0274
33	0.2000/0.1999	0.2003/0.2006	1.0287/1.0275	1.0287/1.0274

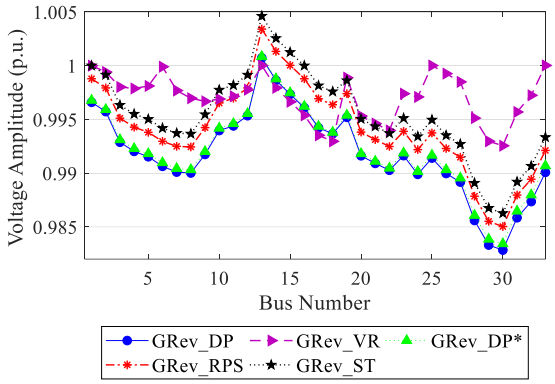

Fig. 2. Test I: Voltage profile of the 33-bus radial microgrid.

- Fig. 1 and Fig. 2 show that the voltage profiles of Test I (radial microgrid) and Test II (meshed microgrid) are identical to those in [3] and [8]. The P/F and Q/V droop coefficients inversely calculated from the droop control (DP) mode (see Table II) equal to the preset values in Tests I/II, which further validates the correctness of GRev.
- Both RPS and ST modes can realize the power sharing goal because DERs adopt the same reactive power ratio. For instance, the DERs share the same $\rho = 1.0287$ under the RPS mode in Test I, which leads to the same var injections of 0.93 p.u.
- In the VR mode, voltages at the DER buses can be restored to the nominal values. However, this causes non-uniform DER var injections. For instance, the minimum and maximum var injections in Test I are 0.03 and 2.93 p.u., respectively. Thus, only with adequate var capacities a microgrid is suggested to work under the VR mode.

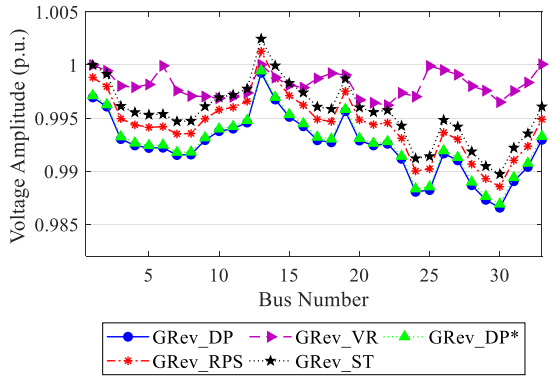

Fig. 3. Test II: Voltage profile of the 33-bus meshed microgrid.

TABLE III
CPU TIME AND ITERATION NUMBERS

	Parameters	DP(I)/(II)	RPS(I)/(II)	VR(I)/(II)	ST(I)/(II)
GRev	Time(s)	0.016/0.012	0.005/0.004	0.029/0.026	0.004/0.004
	Iteration No.	78/72	8/8	86/68	8/8
EMPF	Time(s)	0.50/0.48	0.55/0.54	0.82/0.87	0.80/0.83
	Iteration No.	5/4	10/10	16/16	15/15
GMPF	Time(s)	-/-	0.0316/-	0.0625/-	0.0156/-
	Iteration No.	-/-	9/-	173/-	9/-

B. GRev Results Under Various Structures

Voltages through Tests I and II are shown in Figs. 2 and 3, respectively. It can be seen that:

- The voltage profile in the meshed microgrid is better than its radial counterpart. For example, in the VR mode, the voltage at bus 18 in Test II is 0.9987 p.u. which is 0.53% higher than that in Test I, because bus 18 can receive power support from DER 33 through the link 18-33.
- Load droops can relieve the voltage drops to some extent. In the DP* mode, if we consider the load droop characteristics (droop coefficients for loads 7, 24, 30 and 32: $\mathbf{m_L} = \mathbf{n_L} = [10, 10, 5, 5]^T$), the voltage at bus 32 would be 0.9879 p.u. which is 0.0006 p.u. higher than that without load droop.

From Table III we can see, compared with [3], GRev prevails over GMPF because it is able to handle both radial and meshed structure, whereas GMPF is based on BFS and thus can only solve radial or weakly meshed power flow. Further, GRev is more advantageous than EMPF [8] in terms of the computational speed. Under the same testing condition (ST mode of Test II), GRev is about 200 times faster than EMPF (0.004 s vs 0.83 s [8]). This is because GRev is a derivative-free approach which avoids updating the Jacobian matrix at each iteration.

IV. CONCLUSION

A GRev algorithm is devised to incorporate hierarchical control into the microgrid power flow solution. Case studies validate the efficacy and effectiveness of GRev for both radial and meshed microgrids. Due to its robustness and efficiency, GRev will underpin the microgrid energy management system and will be extended for the power flow analysis of networked microgrids.

REFERENCES

[1] G. Díaz, J. Gómez-Aleixandre, and J. Coto, "Direct backward/forward sweep algorithm for solving load power flows in ac droop-regulated microgrids," *IEEE Trans. Smart Grid*, vol. 7, no. 5, pp. 2208–2217, Sep. 2016.

[2] P. Zhang, *Networked Microgrids*. Cambridge, U.K.: Cambridge Univ. Press, 2020.

[3] L. Ren and P. Zhang, "Generalized microgrid power flow," *IEEE Trans. Smart Grid*, vol. 9, no. 4, pp. 3911–3913, Jul. 2018.

[4] F. Mumtaz, M. H. Syed, M. A. Hosani, and H. H. Zeineldin, "A novel approach to solve power flow for islanded microgrids using modified newton raphson with droop control of DG," *IEEE Trans. Sustain. Energy*, vol. 7, no. 2, pp. 493–503, Apr. 2016.

[5] R. D. Zimmerman, "Comprehensive distribution power flow: modeling, formulation, solution algorithms and analysis," Ph.D. dissertation, Cornell Univ. New York, Ithaca, NY, United States, 1995.

[6] J. W. Simpson-Porco, Q. Shafiee, F. Dörfler, J. C. Vasquez, J. M. Guerrero, and F. Bullo, "Secondary frequency and voltage control of islanded microgrids via distributed averaging," *IEEE Trans. Ind. Electron.*, vol. 62, no. 11, pp. 7025–7038, Nov. 2015.

[7] M. E. Baran and F. F. Wu, "Network reconfiguration in distribution systems for loss reduction and load balancing," *IEEE Trans. Power Del.*, vol. 4, no. 2, pp. 1401–1407, Apr. 1989.

[8] F. Feng and P. Zhang, "Enhanced microgrid power flow incorporating hierarchical control," *IEEE Trans. Power Syst.*, vol. 35, no. 3, pp. 2463–2466, May 2020.